Uncertainties Inherent from Large-Scale Climate Projections in the Statistical Downscaling Projection of North Atlantic Tropical Cyclone Activity

Dazhi Xi[1,2], Ning Lin[1,3], Renzhi Jing[4,5], Patrick Harr[6], Michael Oppenheimer[7, 8, 9]

1. Department of Civil and Environmental Engineering, Princeton University

2. Program in Atmospheric and Oceanic Sciences, Princeton University

3. Andlinger Center for Energy and the Environment, Princeton University

4. School of Medicine, Stanford University

5. Woods Institute of the Environment, Stanford University

6. Jupiter Intelligence

7. School of Public and International Affairs, Princeton University

8. Department of Geosciences, Princeton University

9. High Meadows Environmental Institute, Princeton University

Corresponding Author: Dazhi Xi (dxi@princeton.edu)

Abstract

North Atlantic tropical cyclone (TC) activity under a high-emission scenario is projected using a statistical synthetic storm model coupled with nine Coupled Model Intercomparison Project Phase 6 (CMIP6) climate models. The ensemble projection shows that the annual frequency of TCs generated in the basin will decrease from 15.91 (1979-2014) to 12.16 (2075-2100), and TC activity will shift poleward and coast-ward. The mean of lifetime maximum intensity will increase from 66.50 knots to 75.04 knots. Large discrepancies in TC frequency and intensity projections are found among the nine CMIP6 climate models. The uncertainty in the projection of wind shear is the leading cause of the discrepancies in the TC climatology projection, dominating the uncertainties in the projection of thermodynamic parameters such as potential intensity and saturation deficit. The uncertainty in the projection of wind shear may be related to the different projections of horizontal gradient of vertically integrated temperature in the climate models, which can be induced by different parameterizations of physical processes including surface process, sea ice, and cloud feedback. Informed by the uncertainty analysis, a surrogate model is developed to provide the first-order estimation of TC activity in climate models based on large-scale environmental features.

1. Introduction

Global warming due to increasing greenhouse gas emissions will more likely than not lead to changes in tropical cyclone (TC) climatology. Numerous studies have reported findings about TC climatology change under climate change, with most of the studies reporting TC intensity and rainfall to increase (Knutson et al. 2010; Knutson et al. 2020; Woodruff et al. 2013; Sobel et al. 2016); however, previous studies disagree on how TC frequencies will evolve with climate change (Knutson et al. 2010; Emanuel 2013; Knutson et al. 2020; Lee et al. 2020; Sobel et al. 2021; Jing et al. 2021, Chand et al. 2022). Specifically for the North Atlantic basin, according to the review by Knutson et al. (2020), most studies reported a decrease in North Atlantic TC frequency. I Increases are reported by the downscaling studies of Emanuel (2013) and a few numerical climate models (e.g. Sugi et al. 2009, Bhatia et al. 2018) and there is no agreement on whether the resolution of the models influences the changes in TC frequency (Knutson et al. 2020).

Overall, uncertainties in TC climatology projections are large. As summarized by Knutson et al. (2020), projected change in TC intensity, as represented by the maximum wind speed, in the North Atlantic basin ranges from -9.28% to +20%, and projected changes in North Atlantic TC frequency are within -80% to +222%. However, these large ranges of changes were projected by a number of studies using different projection methods (i.e., direct global climate simulations, regional dynamic climate downscaling, and statistical-dynamic downscaling), different climate model resolutions (14 km-200 km), and different environmental forcings (i.e., increase of CO_2 only, RCP scenarios in CMIP3 and CMIP5, and specified sea surface temperature changes). The abovementioned studies merged uncertainties that originated from multiple sources, including climate simulations and different downscaling approaches, which prohibited a clearer understanding on how the uncertainties in the simulated large-scale environmental features from different climate models influence the uncertainties in TC activity projection. Jing et al. (2021) investigated the discrepancies between climate projections of TC activity using different projection methods, including high resolution climate models, statistical-dynamic downscaling, and statistical downscaling, under the same large-scale environmental forcing. They found that the statistically downscaled TC activity is less sensitive to climate change compared to the statistical-dynamic approach and high-resolution numerical simulation. In this study we aim to investigate the discrepancies/uncertainties in TC climatology projections induced by the uncertainties in large-scale climate features simulated by different climate models.

To perform such analysis, we use the large-scale environment simulated by each of nine CMIP6 climate models (CANESM, CESM2, CNRM, ECEARTH, IPSL, MIROC, MPI, MRI, UKMO) with SSP5 8.5 forcings to drive a statistical synthetic storm model, the **P**rinceton **e**nvironment-dependent **p**robabilistic tropical **C**yclone model (PepC; Jing and Lin, 2020), to simulate a large number of synthetic TC events in the North Atlantic basin from 1979 to 2100. We selected these nine CMIP6 models in order to facilitate future studies to compare PepC downscaling results with several previous studies (e.g. Emanuel 2021, Xi et al. 2023) that downscaled these climate models. Consistently focusing on a specific model subset would allow examination of bias in projections. PepC is a set of statistical models that simulates TC genesis, movement and intensity evolution based on their statistical relationships with the large-scale environment. PepC has been validated with historical observations (Jing and Lin, 2020), and it has been applied to the analysis of TC climatology change (Jing et al. 2021) and landfalling TC rainfall hazards (Xi and Lin, 2022). The advantages of adopting a synthetic storm model are two-fold: (1) the model can be used to efficiently simulate a large number of TC events to support statistically reliable results; (2) it is more flexible and straightforward to perform sensitivity tests using the synthetic storm model than dynamic climate simulations to understand how the uncertainties in the projections of different large-scale environmental parameters propagate to the projections of TC activity.

The study is designed as follows. We couple PepC with each of the nine CMIP6 climate models to perform projections of North Atlantic TC activity; description of the model, method and data are included in Section 2. We first investigate the ensemble mean of the nine downscaling projections to understand the overall trend and the causation of TC climatology changes (Section 3). Then we examine the downscaling results from each individual climate model. To understand how different environmental parameters influence the projected TC activity, we perform sensitivity tests by changing only one large-scale environmental parameter at a time and rerun the simulations (see method and Section 4). Based on the findings in the sensitivity study, we identify the basic large-scale environmental parameters that have strong influences on TC activity. We then build a statistical surrogate model that can be used to provide a first-order estimation of basin-wide TC activity directly from the basic large-scale environmental features, to facilitate climate model selection in TC downscaling analysis (Section 5). We summarize the results of the study in Section 6.

2. Data, Models, and Analysis Methods

The monthly environmental parameters required to drive PepC simulations include atmospheric temperature, humidity, deep layer wind shear, steering wind, low level vorticity, depth of ocean mixing layer, and below-mixing-layer stratification (see Jing and Lin, 2020 for details). These monthly environmental parameters are obtained from the nine CMIP6 climate models. Two simulations from the CMIP6 models are employed in this study: the simulations based on historical forcings from 1979-2014 (hereafter control simulation) and the simulations based on SSP5 8.5 forcings from 2015-2100 (hereafter SSP5 8.5). We noticed that previous research has reported that SSP5 8.5 scenario is unrealistically high in the degree of global warming (Hausfather and Peters, 2020). However, the main point of this study is to reveal the sensitivity of PepC to climate forcings and examine the propagation of uncertainty from climate model simulations to the TC activity projections. The SSP5 8.5 scenario can induce larger projected changes and larger differences among climate model projections, so we select this scenario for analysis in order to facilitate our study. Projection of TC climatology and hazards under other scenarios are left for future research. To account for possible biases in climate model projections, we bias correct the simulated large-scale environmental parameters in each climate model by adding the monthly differences between reanalysis dataset (ERA5) and the control simulation by the climate models (both averaged over the period of 1979-2014). The reason we bias-correct the climate models toward ERA5 is that the PepC model is trained based on the ERA5 reanalysis environment.

PepC consists of three parts: a genesis model, a track model, and an intensity model. PepC simulates TC genesis using a cluster-Poisson regression model. In PepC, TC geneses are forced by four parameters: environmental maximum potential intensity (V_p), deep layer wind shear (Shear, calculated as the wind velocity difference between 200 hPa and 850 hPa), mid-troposphere saturation deficit (also known as entropy deficit, SD), and 850 hPa absolute vorticity (VO850). The low-level vorticity represents the influence of initial disturbances, and the other parameters in the genesis model describe how a favorable environment supports the development of initial disturbances into TCs. The original PepC model in Jing and Lin (2020) used relative humidity as the atmospheric humidity parameter and they discussed the possibility of using SD for genesis modeling. Although using relative humidity in the genesis model yields better performance of PepC in reproducing the interannual variability of genesis frequency in the historical observations, SD is theoretically related to the time that an initial vortex takes to evolve into a TC (Emanuel et al. 2008). Thus, in this study we choose to use SD to represent atmospheric humidity in projecting future TC genesis. Grids in the Norh Atlantic basins are first clustered based on these environmental parameters, then in each cluster the monthly genesis frequency is simulated based on a Poisson regression model. Different from the synthetic storm model developed by Emanuel et al. (2006) who adopted constant seeding rate, the seeding rate in PepC is related to the abovementioned environmental parameters.

After a TC seed is generated, it is moved by the analog-wind track model. Horizontal wind in 850 hPa and 200 hPa, as well as the movement of a TC in the previous steps are used to predict the movement of TCs. Along each simulated track, intensity of the TC is modeled by an environmental-dependent hidden Markov Chain (Jing and Lin 2019) given Vp, Shear, relative humidity (RH), and oceanic parameters (OP). The lifetime of a TC is separated into three states and the transition between different states is modeled as a Markov Chain with the transition matrix estimated based on the environmental parameters; meanwhile, the intensity change is predicted using different regression models that link 6-hour intensity change with environmental parameters for different states. Detailed description of PepC model can be found in Jing and Lin (2020). PepC is used to simulate North Atlantic TCs from 1979-2100 forced by bias-corrected environments from the CMIP6 models. For each climate model, simulations are performed ten times to generate a large sample. The total number of TCs generated by each CMIP6 climate model is summarized in Table S1.

To investigate how uncertainties in the projection of the large-scale environmental parameters influence the projection of TC activity, we performed a series of sensitivity analyses. The sensitivity of TC activity to each individual selected variable is defined in each CMIP6 model by altering each variable from the 36-year control simulation to the final 36-year SSP5 8.5 simulation (2065-2100) while holding all other variables to their original (control simulation) values. TC genesis and intensity are projected to have larger changes under climate change compared to TC track (Section 3), accordingly, we focus on the sensitivity analysis of TC genesis and intensity. We test the influence from each of the environmental parameters (Vp, Shear, SD, VO850) on TC genesis using the abovementioned methodology. For TC intensity, Vp , Shear, OP (calculated from mixing layer depth and below-mixing-layer stratification) and high-level relative humidity (RH, averaged between 300 and 500 hPa) are used as predictors and are tested following a similar method; the sensitivity analysis for the intensity is performed based on the tracks simulated from the control simulation in each climate model.

As will be shown in Section 4, the inter-model differences of projected Shear are important to the uncertainty in projected TC activity. Because of the dynamic linkage between deep level wind shear and temperature gradient, we investigate the climate projections of the zonally-averaged vertically-integrated temperature ($Tzp = \int_{\lambda=260}^{\lambda=340} \int_{p=850}^{p=200} \frac{T}{p} dpd\lambda$, where λ represents longitude) and the meridional-averaged vertical-scaled temperature ($Tmp = \int_{\phi=5}^{\phi=35} \int_{p=850}^{p=200} \frac{T}{p} dpd\phi$, where ϕ represents latitude) in different climate models. The range of integration is selected to be consistent with the domain for the wind shear analyses detailed further in Section 4.

Inspired by the abovementioned uncertainty analysis and the need to pre-select a subset of climate models for more reliable downscaling of TC activities in future applications, we developed a statistical surrogate model based on a single-layer neural network model where the annual power dissipation index (PDI), a parameter that represents TC activity, is predicted using basin-averaged environmental parameters including air temperature at 850 hPa, relative humidity at 850 hPa, vorticity at 850 hPa, and vertical wind shear (wind difference between 200hPa and 850 hPa). The shallow neural network consists of an input layer, a 10-neuron hidden layer, and an output layer. Detailed reasons for selecting these predictors and the model performance can be found in Section 5.

3. Ensemble Projections of North Atlantic TC Activities

First, we examine the ensemble mean projection of TC activity. The ensemble projection shows a decrease in North Atlantic storm frequency under the SSP5 8.5 scenario (Figure 1a). In the historical climate (1979-2014), on average 15.91 storms are generated in the North Atlantic basin per year (historically, on average there are 15.41 storms per year in the observation, Jing and Lin, 2020), while the number decreases to 12.16 during the last 36 years of the 21st century (2065-2100). The mean genesis frequencies in the two periods are significantly different at the 5% level based on a two-sample t-test. In the historical climate, there are four main regions in which TCs form: west of Africa, north of South America, northern part of the Gulf of Mexico, and east of Florida Peninsula (Figure 1b). The end-of-century projections indicate that the proportion of storms generated in the northern part of the Gulf of Mexico and east of Florida Peninsula will increase, while the proportion of storms in the west of Africa and north of South America will decrease (Figure 1c). Therefore, there will be proportionately larger number of TCs form close to the US coastlines. These patterns can also be seen via the track density plot (Figure 1d, 1e), which identifies proportionally higher TC activity near the US coastlines by the end of this century even though less storms are generated across the North Atlantic basin. Additionally, in the future, proportionally more storms will reach their lifetime maximum intensity (LMI) along the Gulf coast and to the east of Florida Peninsula (Figure 1f, 1g). Also, storms will become more intense by the end of this century, with the probability distribution of storm LMI shifting towards higher values (Figure 1h). In the historical climate, the mean (90-th percentile) of the storm LMI averaged over 1979-2014 is 66.50 knots (111.47 knots), and it increases to 75.04 knots (125.03 knots) in 2065-2100 (Figure 1h). The mean LMI in the two periods are significantly different at the 5% level based on a two-sample t-test.

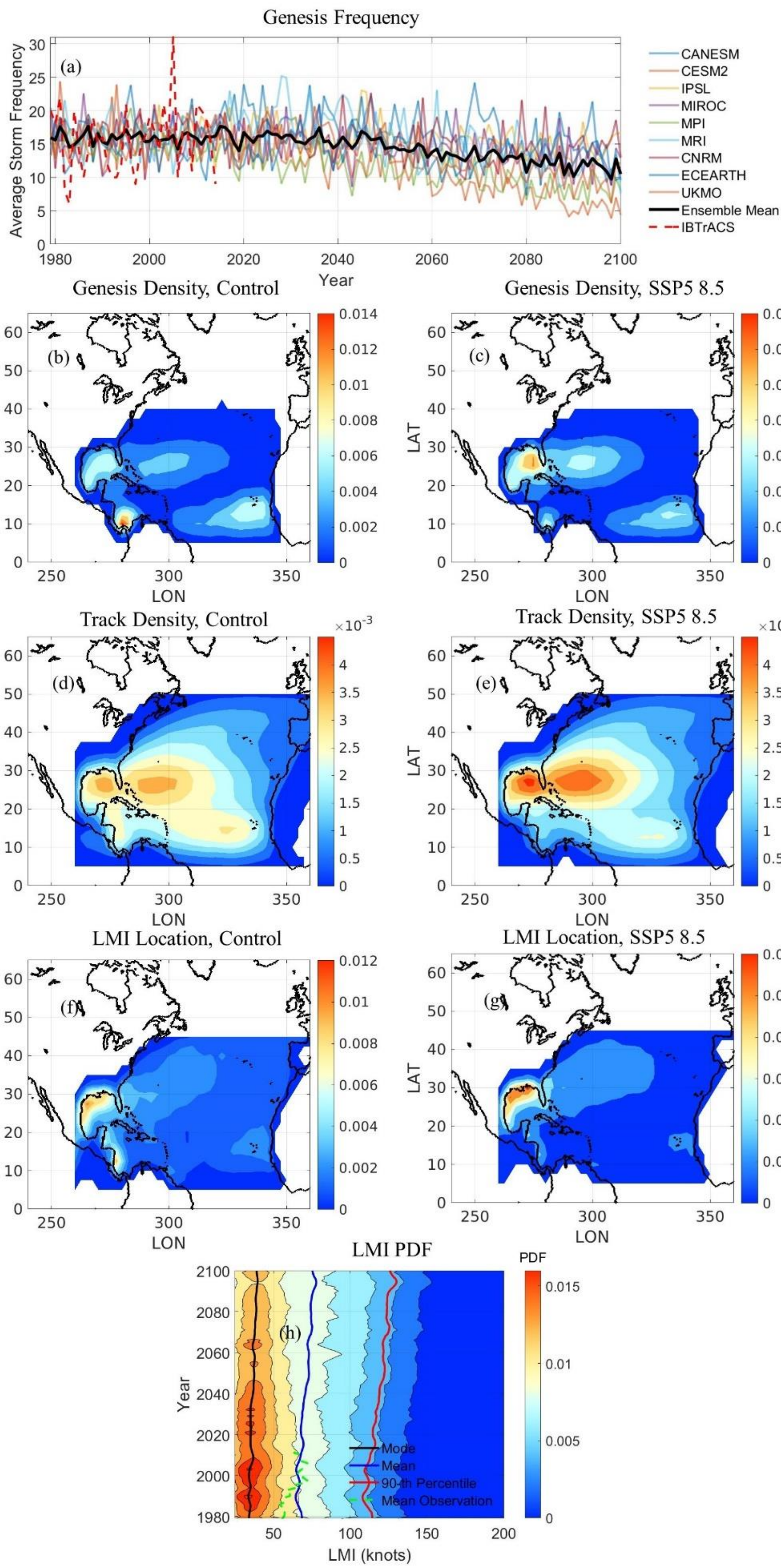
Genesis Frequency
(a)
Average Storm Frequency
Year
CANESM
CESM2
IPSL
MIROC
MPI
MRI
CNRM
ECEARTH
UKMO
Ensemble Mean
IBTrACS
Genesis Density, Control
Genesis Density, SSP5 8.5
(b)
(c)
LAT
LON
Track Density, Control
Track Density, SSP5 8.5
(d)
(e)
×10^-3
LMI Location, Control
LMI Location, SSP5 8.5
(f)
(g)
LMI PDF
(h)
PDF
Mode
Mean
90-th Percentile
Mean Observation
LMI (knots)

Figure 1. Ensemble projection of TC activity in the North Atlantic basin. (a) annual storm frequency in the North Atlantic basin from 1979-2100. (b)(c) annual genesis density averaged over 1979-2014 and 2065-2100, respectively. (d)(e) annual track density averaged over 1979-2014 and 2065-2100, respectively. (f)(g) annual frequency of storms achieving lifetime maximum intensity (LMI) in the $2.5^{o} \times 2.5^{o}$ grid boxes averaged over 1979-2014 and 2065-2100, respectively. In Figure b-g, values are first calculated in $2.5^{o} \times 2.5^{o}$ grid boxes and then scaled by the summation of the values in all grid points to better show the spatial pattern. (h) probability density function (PDF) of LMI from 1979-2020. The black line shows the mode of the LMI probability distribution (mode is the LMI value at which its probability density function has the maximum value), the blue line shows the mean of the LMI, and red line shows the 90-th percentile of LMI. The green dashed line shows the mean LMI in observation.

The projected changes in TC climatology can be understood by examining the changes of large-scale parameters that drive the simulation of TC frequency, intensity, and track in PepC (Figure. 2). Equatorward of 15ºN, Vp changes (Figure. 2a-c) are within $\pm$5 kt. At higher latitudes (15ºN - 35ºN), Vp increases are larger, which explains the northward shift of TC activity in the future. SD increases across the basin (Figure. 2d-f), which is consistent with previous research (Lee et al., 2020). Over all the locations where TCs primarily form in the control simulation, the Caribbean Sea north of South America experiences the largest increase in SD, which corresponds to the largest decrease in TC genesis there (Figure. 1b-c). Wind shear increases over the Caribbean Sea north of South America (Figure. 2g-i), which also contributes to the decrease in TC formation over that area (Figure. 1b-c). The decrease in wind shear near North America, which has been discussed in several previous research (Ting et al. 2019, Balaguru et al. 2023), contributes to the increase in TC formation in that area (Figure. 1b-c). The low-level vorticity (Figure 2j-l) increases slightly through the Caribbean Islands and in the current main development region (around 10º N west of Africa). However, the mid-level relative humidity slightly decreases over both the Caribbean and strongly decreases over the main development region. Therefore, changes in all variables favor the northward shift of TC formations (Figure. 1b-c) and tracks (Figure. 1d-e) in the North Atlantic basin and a general shift toward North America continent.

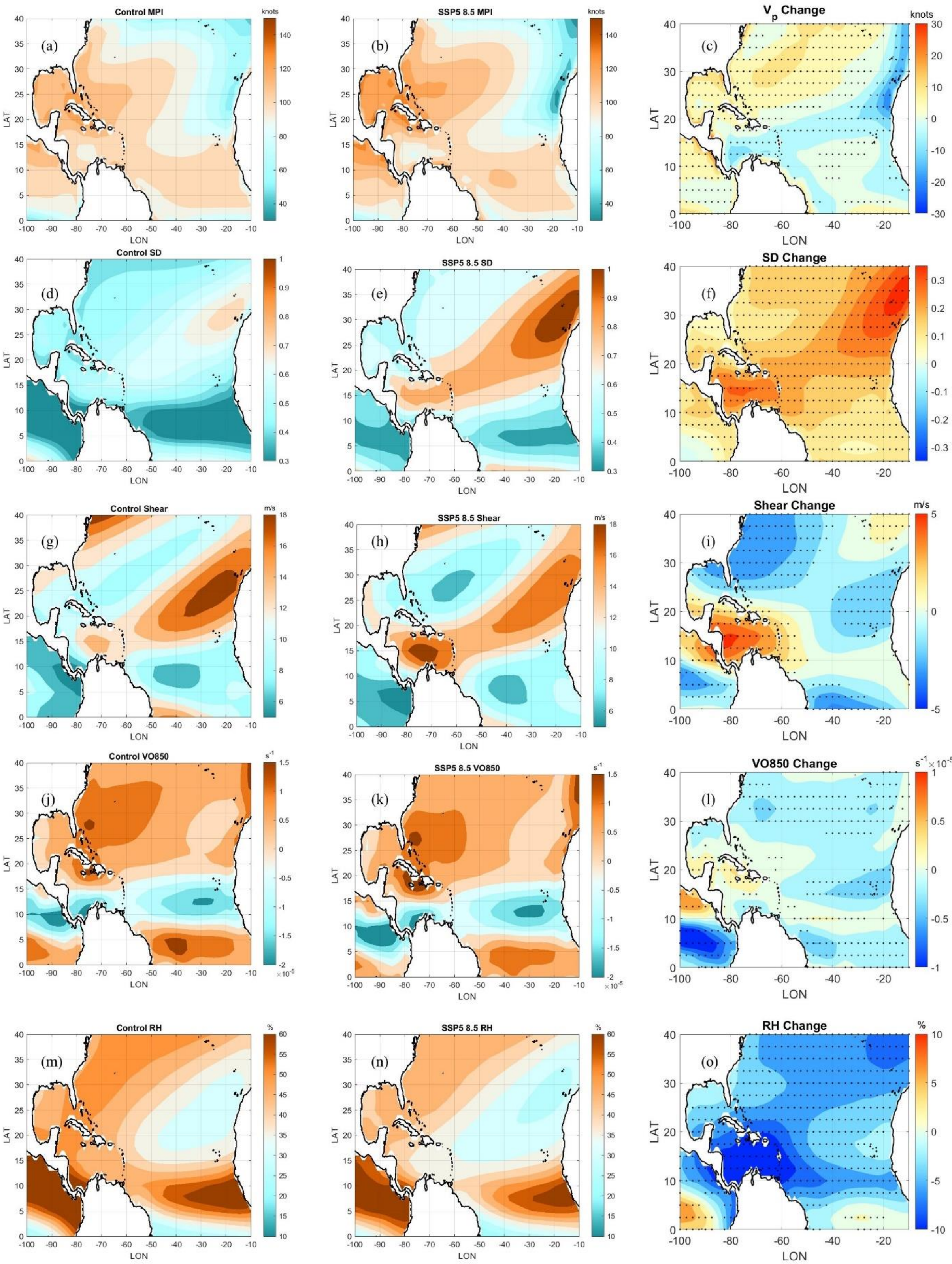

Control MPI
knots
(a)
SSP5 8.5 MPI
knots
(b)
V_p Change
knots
(c)
Control SD
(d)
SSP5 8.5 SD
(e)
SD Change
(f)
Control Shear
m/s
(g)
SSP5 8.5 Shear
m/s
(h)
Shear Change
m/s
(i)
Control VO850
s^-1
(j)
SSP5 8.5 VO850
s^-1
(k)
VO850 Change
s^-1 ×10^-5
(l)
Control RH
%
(m)
SSP5 8.5 RH
%
(n)
RH Change
%
(o)
LAT
LON

Figure 2. Changes of environmental variables that influence TC activity in PepC, averaged during North Atlantic TC season (July-October) and across the nine CMIP6 models. The first column shows the variables in the control simulation (1979-2014), the second column shows the variables in SSP5 8.5 (2065-2100), the third column shows the change (future period minus historical period). (a)(b)(c). Maximum potential intensity; (d)(e)(f). saturation deficit; (g)(h)(i). deep layer wind shear; (j)(k)(l). low level vorticity (850 hPa); (m)(n)(o). high level relative humidity (300 hPa – 500 hPa). The dots in the right column indicate the locations where the difference passes the two-sample t-test under the 5% significance level.

4. Uncertainties Inherent from Climate Projection

Though the ensemble results show a clear trend of decreasing TC frequency and increasing TC intensity in the North Atlantic basin, there are discrepancies among different CMIP6 climate models. For example, the ensemble mean defines a decrease in TC genesis frequency, but the CANESM model projects a slight increase (Figure 1a, Table S2). The CNRM model projects an increase in TC genesis west of Africa (Figure 3a, 3b) though the ensemble mean defines a decrease in frequency in that region (Figure 1b, 1c, Figure 3a, 3b). Differences among models can also be found in track density projections. Although the ensemble mean projection defines a decrease in TC activity in the west of Africa (Figure 1d, 1e), the CNRM model projects an increase in TC activity in that region (Figure 3c, 3d). There are also differences among other models (Figures S1, S2), for example, CANESM model projects relatively more storms generated near US coastline than other models, and CESM2 model projects the most significant TC activity decrease in the North Atlantic basin among the nine selected models. Although the change in locations of LMI does not show significant differences across the nine climate models (Figure S3), there is a large uncertainty in the projection of the probability distribution of LMI, including the mean and 90-th percentile of LMI (Figure 4). For example, CANESM renders the largest change in LMI from control to future projection (+17.19 knots), while CESM2 projects the least increase in LMI (+2.24 knots). Also, some models project larger changes in the thermodynamic parameters of the environment than others, e.g., the MPI model showing the lowest Vp increase (Figure 5) and the CANESM model showing the largest SD increase over the largest spatial extent (Figure 6). The uncertainties in the spatial pattern of change in wind shear, low-level vorticity, and relative humidity are also substantial (Figures 7, 8, 9). For example, MIROC model shows the lowest increase in vertical wind shear in the Caribbean Ocean (Figure 7), and the increase in low-level vorticity in the MIROC model extends to the Northeast coast of the US (Figure 8).

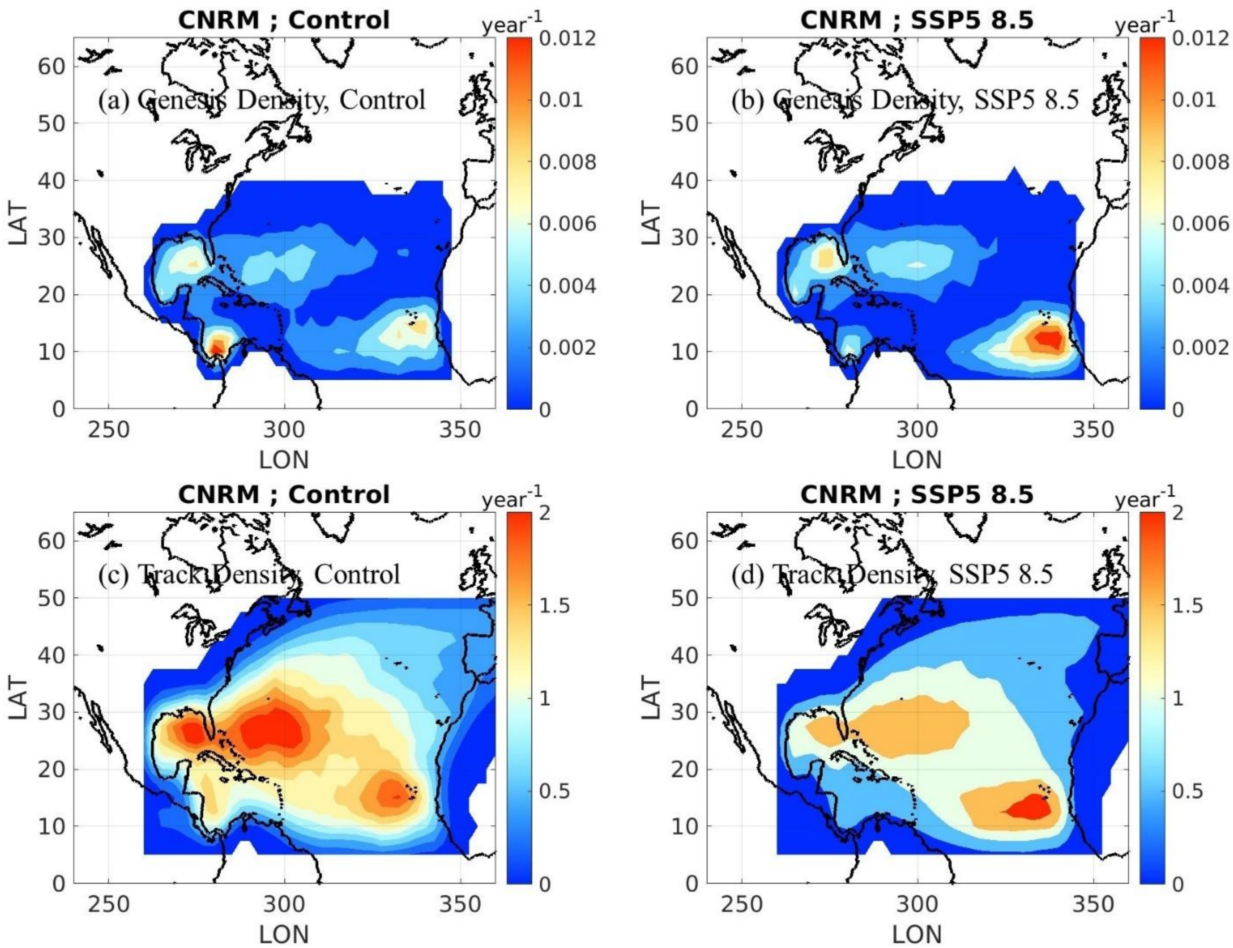

Figure 3. North Atlantic TC genesis density (a, b) and TC track density (c, d) under control climate and SSP5 8.5 forcings in the CNRM model.

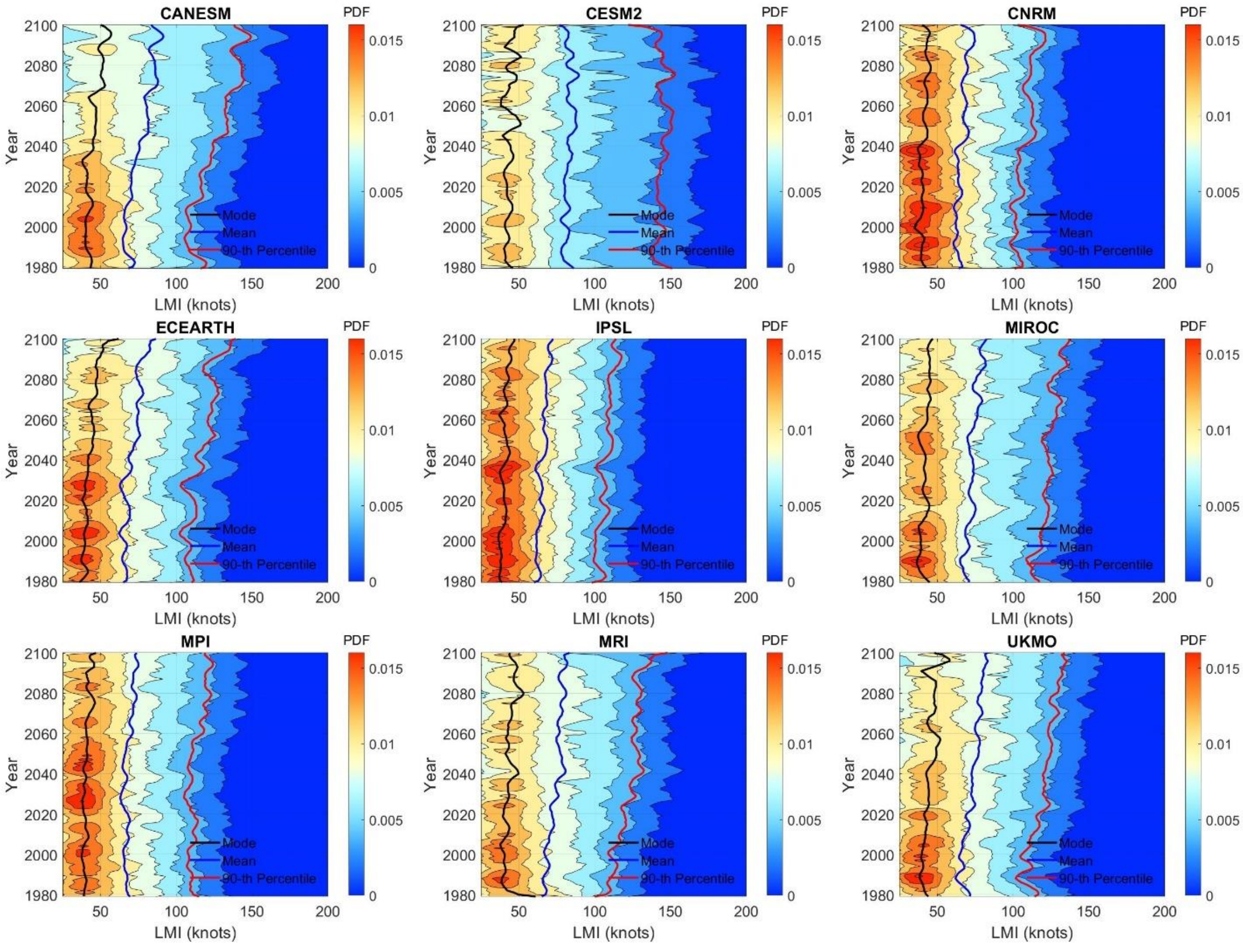

Figure 4. Probability density function (PDF) of annual LMI for each CMIP6 climate model. The black lines show the mode of the LMI probability distribution (mode means the LMI value at which its probability density function has a maximum value), the blue lines show mean of the LMI, and the red lines show the 90-th percentile of LMI.

To test how the uncertainties in TC projections are related to the uncertainties in the simulated large-scale environment, we change the parameters that drive PepC simulations to their values during 2065-2100 one at a time and keep other parameters unchanged as during 1979-2014, and we perform PepC genesis and intensity simulations for each CMIP6 model. The changes in these parameters (Vp, SD, VO850, Shear, and RH) are not significantly correlated with each other (Figure S4). Although some changes appear correlated (e.g., changes in Vp and Shea r), none of the correlations are statistically significant under the 5% level so it is reasonable to perform sensitivity tests of each parameter one at a time.

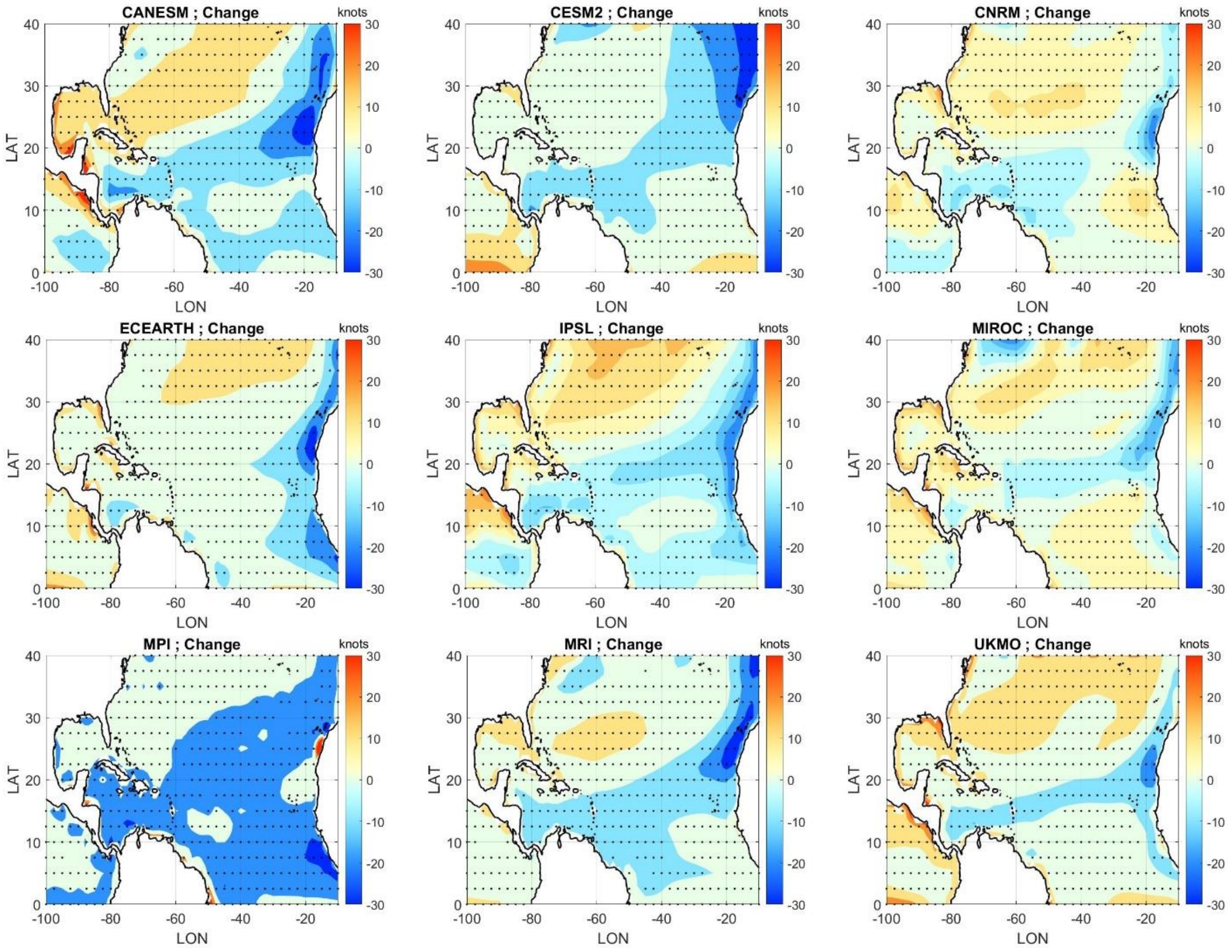

Figure 5. Change of maximum potential intensity (Vp) in each climate model (similar to Figure 2c) from 1979-2014 to 2065-2100. The dots indicate the locations that the difference passes the two-sample t-test under the 5% significance level.

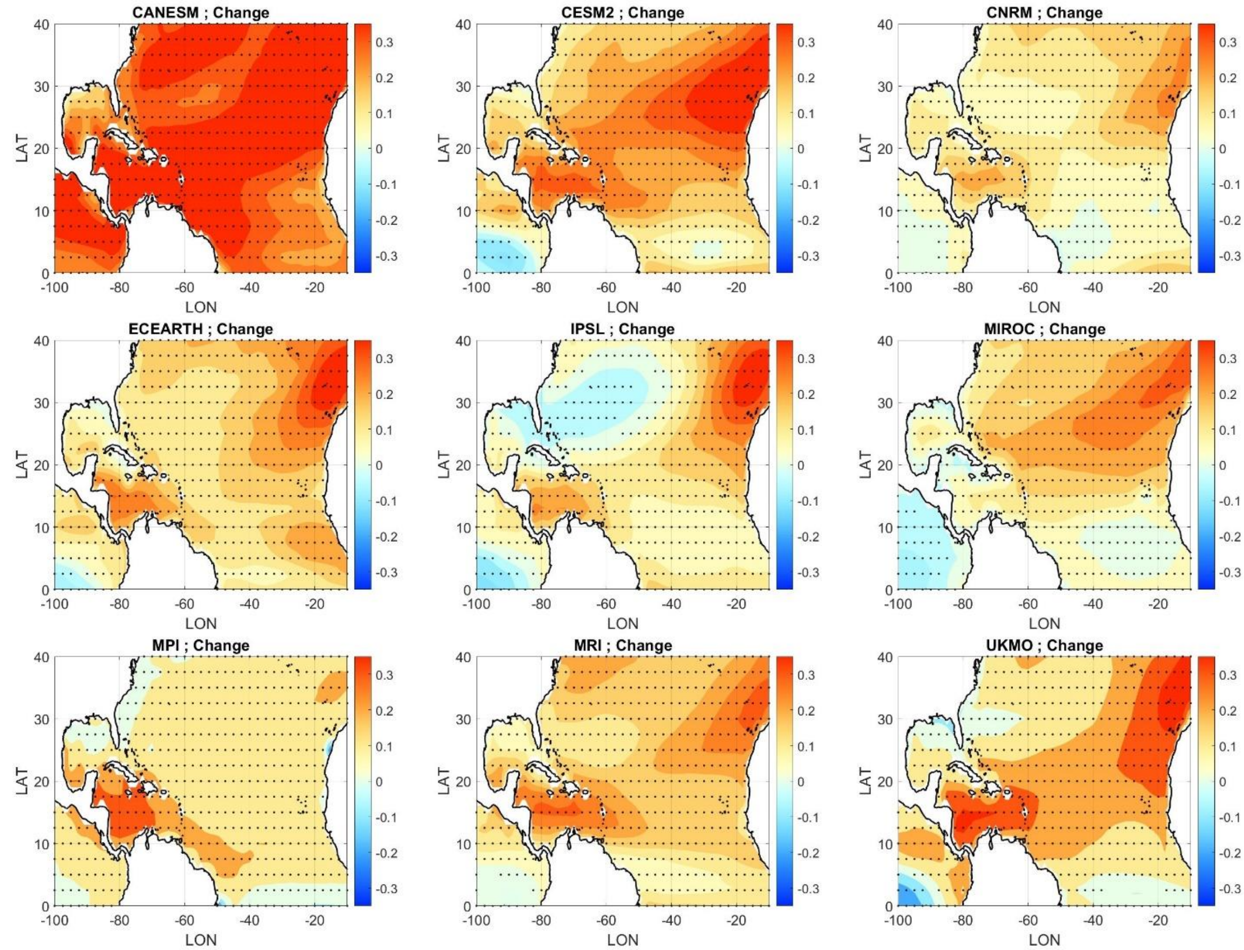

Figure 6. Change of saturation deficit (SD) in each climate model (similar to Figure 2f) from 1979-2014 to 2065-2100. The dots indicate the locations that the difference passes the two-sample t-test under the 5% significance level.

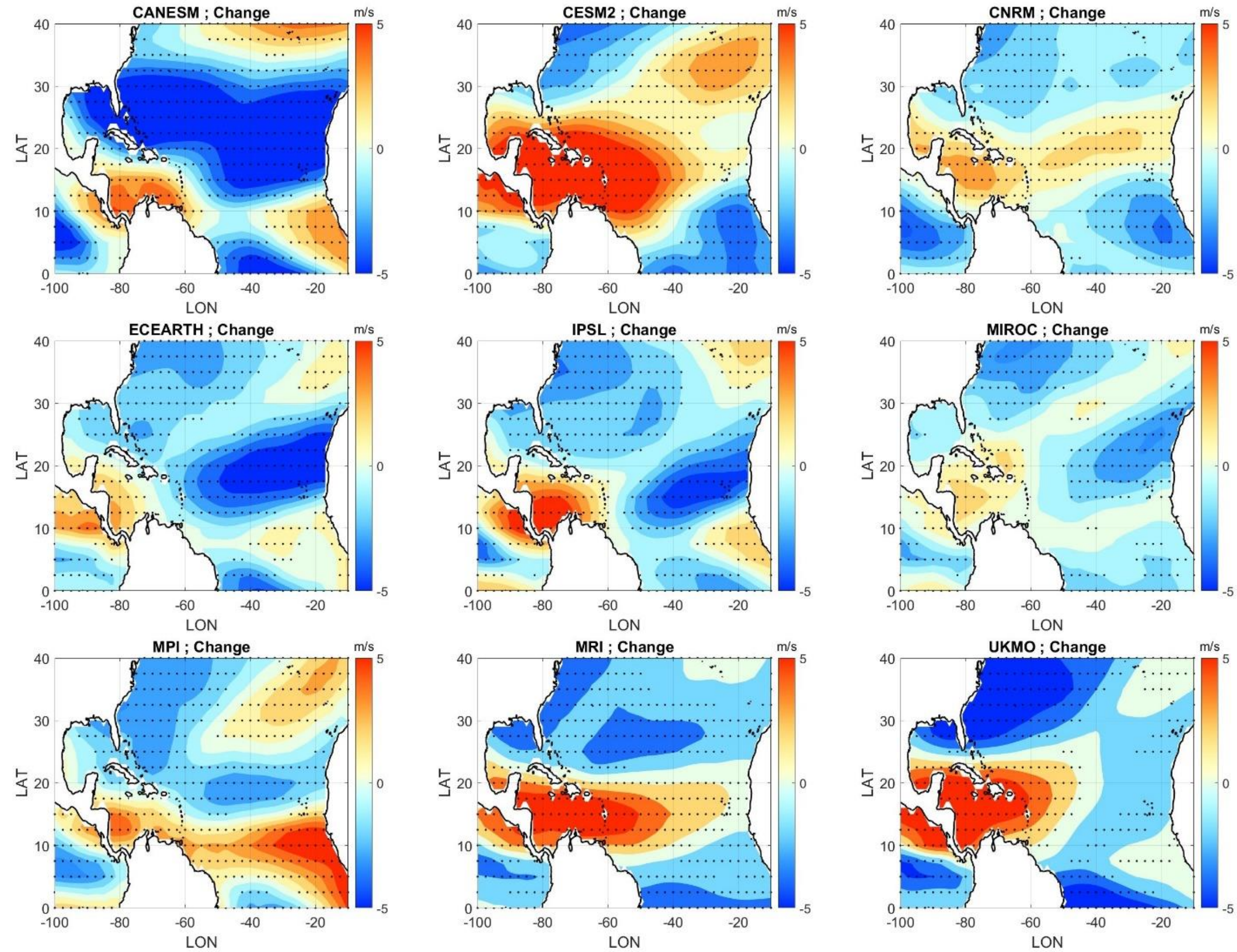

Figure 7. Change of deep level wind shear in each climate model (similar to Figure 2i) from 1979-2014 to 2065-2100. The dots indicate the locations that the difference passes the two-sample t-test under the 5% significance level.

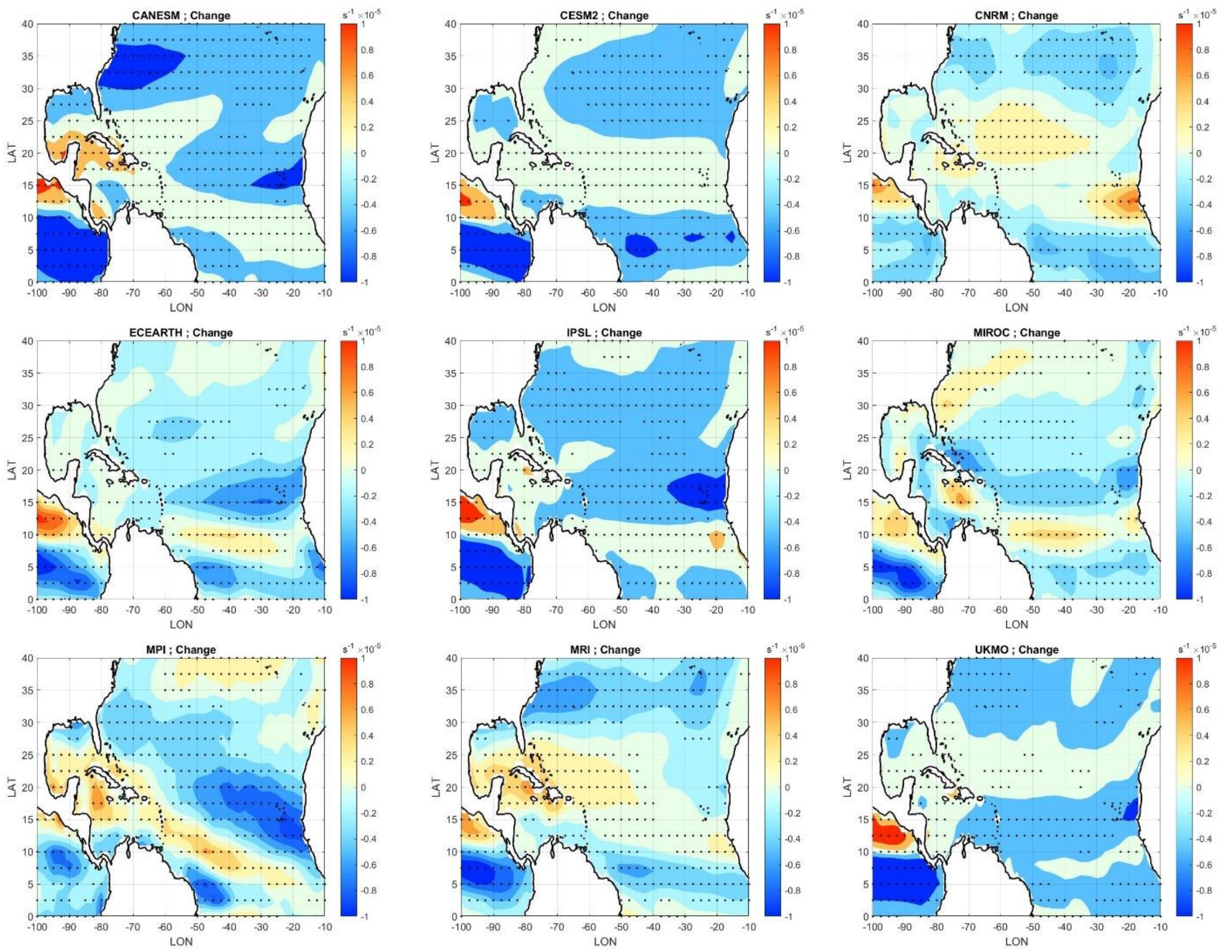

Figure 8. Change of low-level vorticity in each climate model (similar to Figure 2l) from 1979-2014 to 2065-2100. The dots indicate the locations that the difference passes the two-sample t-test under the 5% significance level.

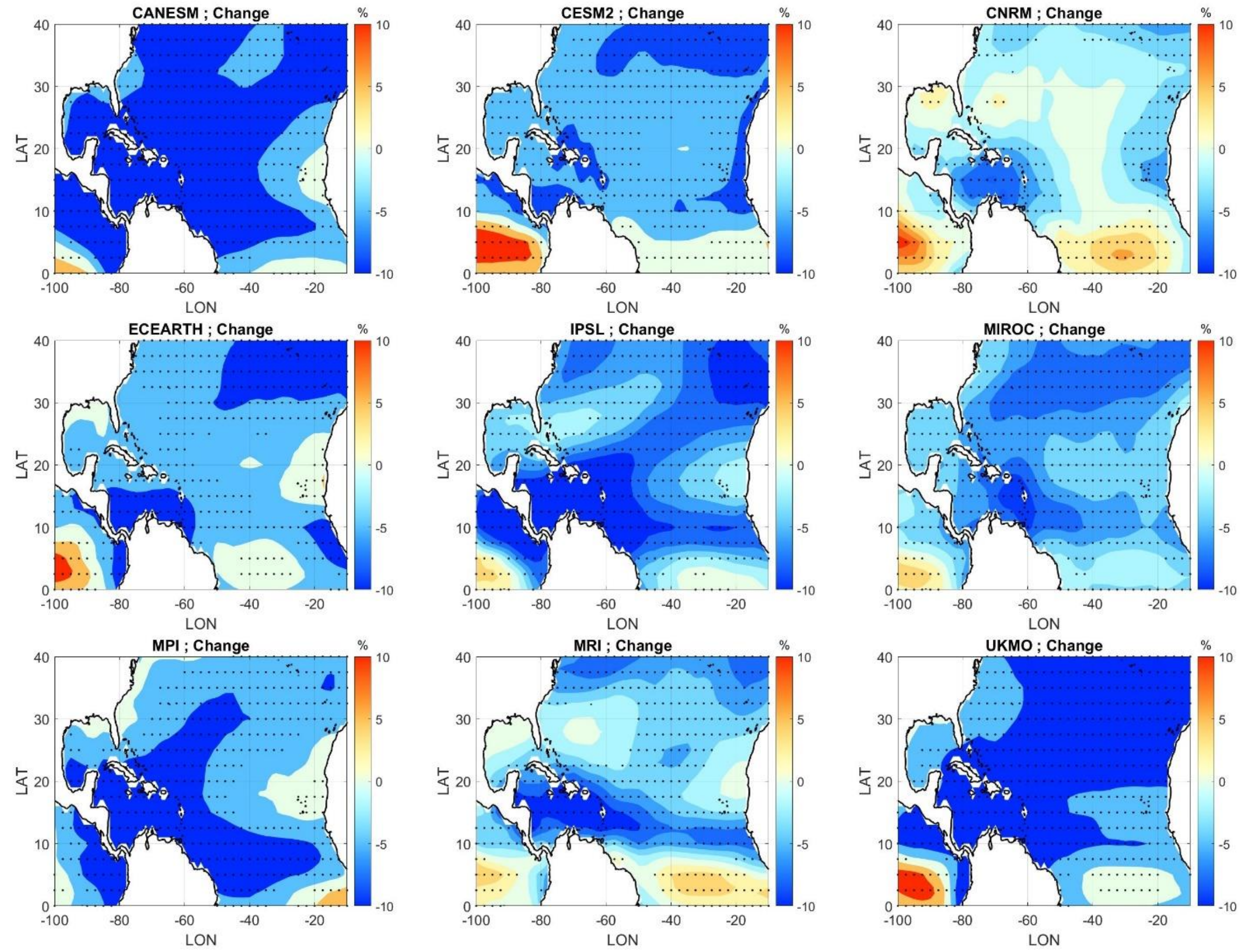

Figure 9. Change of relative humidity in each climate model (similar to Figure 2o) from 1979-2014 to 2065-2100. The dots indicate the locations that the difference passes the two-sample t-test under the 5% significance level.

We first examine how TC frequency changes are influenced by the changes in the parameters that are included in the PepC's genesis model (Vp, SD, SHR, and VO). For TC genesis, except the CANESM model, all other selected CMIP6 models project a decrease trend in TC frequency although the degrees of change are different among the models (black squares in Figure 10). The Vp change from current to end-of-century values causes TC annual frequency to increase (+0.72 to +2.78) in all models except for the MPI model (-0.80, red dots in Figure 10a, Table S2). The change in SD causes a strong decrease in TC frequency (-9.77 to -4.05) and dominates over the influence from other parameters (blue dots in Figure 10a, Table S2). Impacts from changes in Shear and VO850 vary among different climate models. Change in shear causes increase in storm frequency in CANESM (+4.91), IPSL (+0.58), MIROC (+0.21), and ECEARTH (+1.19) but decrease in other models (-0.49 to -3.46). The VO850 change causes TC frequency to increase in CANESM (+2.15), CESM2 (+1.28), IPSL (+0.39), MRI (+0.97), and CNRM (+2.17) models and decrease in other models (-0.15 to – 0.93, Figure 10a, Table S2). Changes in TC frequency caused by changes in Shear have the highest correlation with the change in the SSP5 8.5 simulation (Table 1). The standard deviation of Shear-induced change and VO850-induced change is larger than the mean (Table 1), indicating that the CMIP6 models (coupled with PepC) differ markedly in their projection of the changes in these parameters and thus their effects on future TC frequency changes. Overall, the climate models have larger projection uncertainties/discrepancies in the dynamic parameters (Shear, VO850) than in the thermodynamic parameters (Vp, SD).

For LMI (Figure 10b, Table 2), we analyze the impact from parameters (Vp, OP, RH, and SHEAR) that are included in the intensity model of PepC on the mean LMI change. We found that the change in the ocean parameter has a much smaller influence on LMI change compared to the atmospheric dynamic and thermodynamic parameters. For the thermodynamic parameters, climate models (coupled with PepC) have consistent implications for their influences on LMI. All models indicate that the change in Vp causes an increase in LMI (+1.94 to +11.57), and the increase dominates compared to other parameters (Figure 10b). For the RH change, all models indicate that it causes a decrease in LMI (-1.81 to -0.56; Figure 10b). Similar to the response in TC frequency, the responses in LMI to the change in Shear are different for different models, with positive influence in CANESM (+5.82), IPSL (+1.02), MPI (+0.74) and ECEARTH (+1.66) models and negative influence in other models (-7.61 to -0.35; Figure 10b and Table S3).

The analysis above focuses on the parameters that are included in PepC model. Although other environmental factors (e.g. ventilation index) may also have influence on TC climatology, since they are not included in the PepC model based on the statistical analysis (Jing et al. 2019, Jing and Lin 2020), we focus on the parameters that are used by the PepC model.

Table 1. Change in TC Genesis Frequency Caused by Individual Parameter

	Correlation with SSP5 8.5 Genesis Change across nine CMIP6 models	Averaged Change in Genesis across nine CMIP6 models	Standard Deviation of Change in Genesis across nine CMIP6 models

Vp	0.46	1.42	1.04
SD	0.12	-6.47	1.81
SHR	0.86	-0.06	2.31
VO	0.35	0.52	1.19

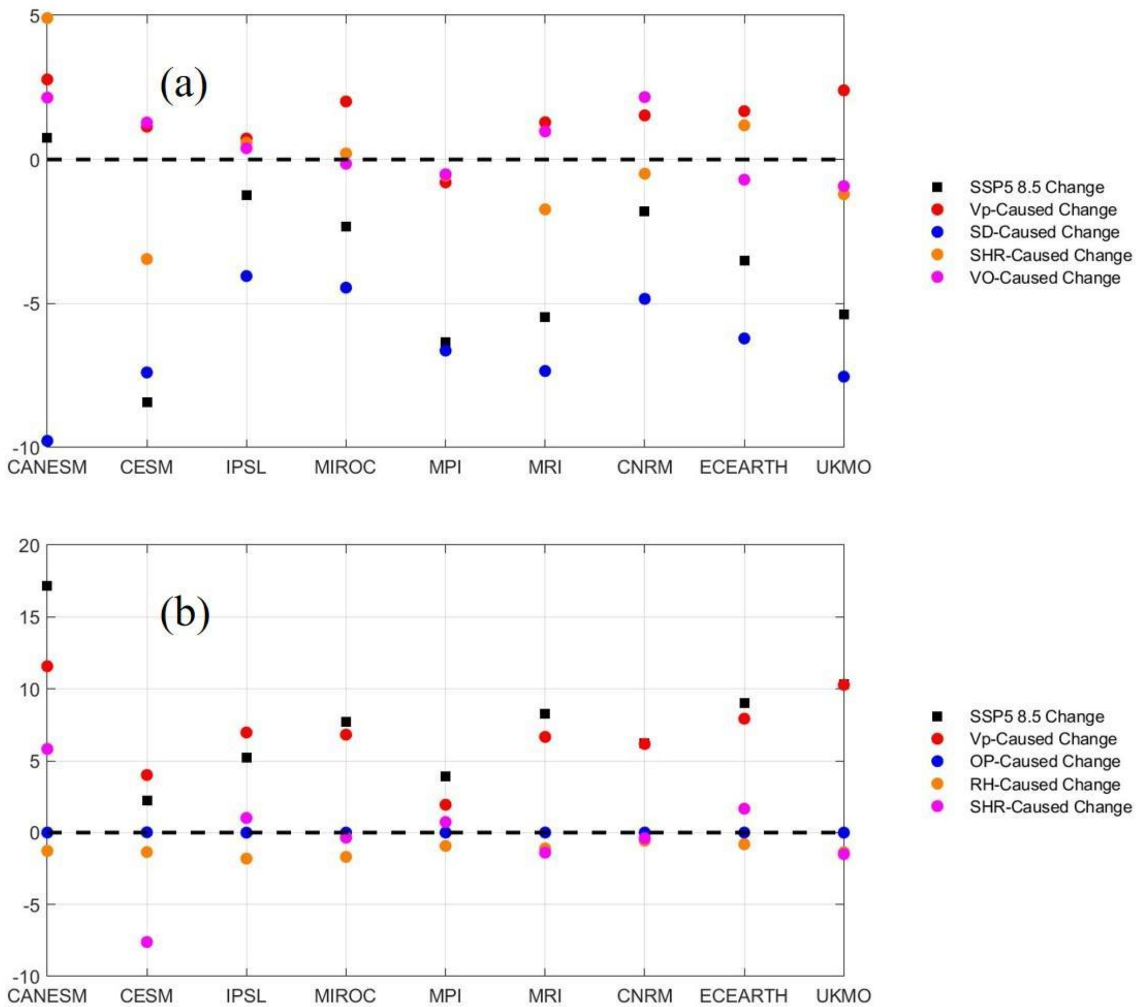

Figure 10. Climate sensitivity tests of the influence of large-scale environmental parameters on TC genesis and intensity. (a). Change of North Atlantic TC frequency caused by the change in each individual parameter. (b). Same as (a). but for LMI. The dashed line indicates the level of no change.

Table 2. Change in TC Mean LMI Caused by Individual Parameters

	Correlation with SSP5 8.5 Mean LMI Change	Averaged Change in Mean LMI across nine CMIP6 models	Standard Deviation of Change in Mean LMI across nine CMIP6 models
Vp	0.89	6.93	2.91
OP	-0.36	0.003	0.01
RH	-0.01	-1.21	0.40
SHR	0.73	-0.22	3.54

The abovementioned analysis implies that the uncertainties in the projection of wind shear across climate models may have profound impact on the projected TC climatology changes. Averaged across the region where we see most of TC activity in the North Atlantic basin (from 5 ^{o}N to 35 ^{o}N and from 100 ^{o}W to 20^{o}W), CESM, MPI, MRI, CNRM, and UKMO models project an increase in wind shear while other models project a decrease (Figure S4). To understand why there are such large uncertainties across different climate models, we examine the changes in vertical shear of zonal wind (Figure 11a) and meridional wind (Figure 11b) separately and link the changes to the zonal and meridional gradient of vertically integrated temperature (Figure 12a, b). In the tropics, though the large-scale circulation is not in (quasi) geostrophic balance so the thermal-wind balance does not hold theoretically, the horizontal temperature gradient can still influence the vertical wind shear. In control simulations, all models show that air is warmer in the tropics and cooler in the subtropic (Figure 12a) and exhibit the valley-shaped zonal distribution of the meridionally averaged temperature (Figure 12b). This spatial distribution is related to the land-sea contrast. Overall, the air temperature on the west side of the North Atlantic basin is higher than the east side. Although the differences between climate models in simulating the air temperature in the control experiment are not large (in terms of both absolute value and the spatial distributions), the models show large uncertainties in air temperature change under climate change (see also Figure S6). For some climate models (and the ensemble average), the tropics are warmed up more than the subtropics while others show more homogeneous warming (Figure 12c, Figure S6). For example, the CESM2 model shows the largest tropic-subtropic contrast in air-warming, which explains why it shows the highest increase in vertical wind shear of zonal wind (Figure 11a). The IPSL, MIROC, MPI models, however, show less tropic-subtropic contrast in air-warming and less vertical shear of zonal wind (Figure 11a). Most of the climate models (and the ensemble average) show more temperature increase in the east part of the North Atlantic basin, and there are positive changes in the vertical shear of meridional wind (Figure 11b). Though this analysis may not be applicable to each individual model (e.g., shear of meridional wind in CESM2) due to the localized temperature gradient and the non-geostrophic nature of tropical atmosphere, the change in the spatial pattern of air temperature still explains the overall uncertainties of projected changes in wind shear. The uncertainties of projected meridional gradient of temperature are reported to be related to the differences in the parameterization in cloud processes and feedback mechanisms in the climate system such as the influence of sea ice (Flato et al. 2014, Pithan and Mauritsen, 2014), and the uncertainties of projected zonal gradient (land-sea contrast) may be related to the different parameterizations of surface processes and ocean dynamics (Karmalkar et al. 2011). Balaguru et al. (2023) also suggests that an increase in diabatic heating in the eastern tropical Pacific and the adjustment of circulation to this forcings are responsible for the decrease in wind shear, and the inter-model uncertainty related to the wind shear change can be attributed to the diabatic heating.

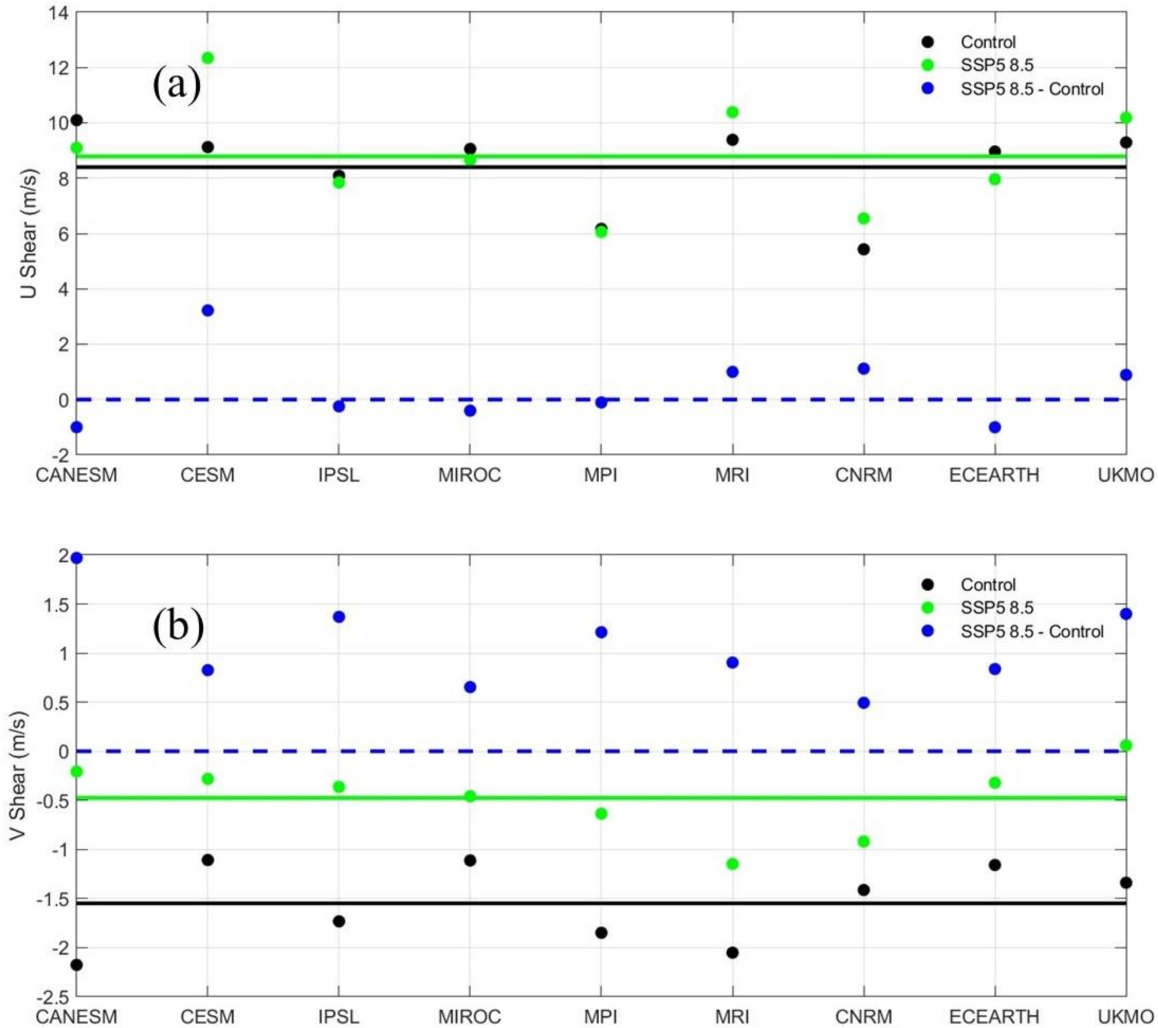

Figure 11. Change of vertical wind shear components over the North Atlantic basin. (a) Change of vertical shear of zonal wind. (b) Change of vertical shear of meridional wind. The dashed blue line indicates the level of no change. The green solid line indicates the averaged SSP5 8.5 wind shear level, while the black solid line indicates the averaged historical wind shear level.

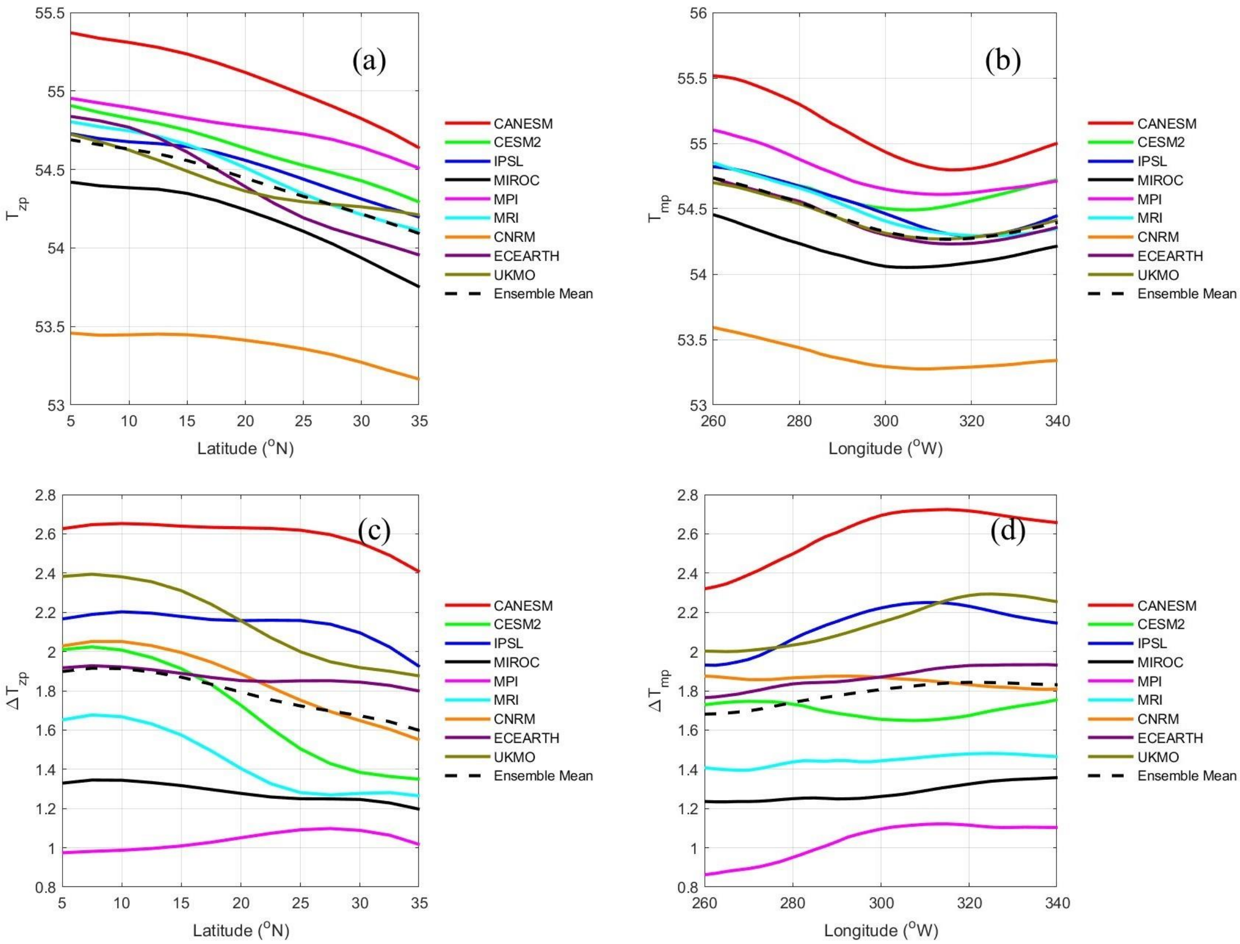

Figure 12. Temperature distribution in the North Atlantic basin. (a) Zonally-averaged vertically-integrated temperature (Tzp defined in section 2) in different climate models in the historical period. (b) Meridionally-averaged vertical-integrated temperature (Tmp defined in section 2) in different climate models in the historical period. (c) Change of the zonally-averaged vertically-integrated temperature. (d) Change of the meridionally-averaged vertical-integrated temperature.

5. Large-scale Environmental Controls of TC Activity

In this and previous TC climate downscaling studies (e.g., Emanuel 2021), projections are presented from a subset of climate models selected mainly based on data availability and the number of models selected are restricted by storage limitations. Thus, the ensemble projections based on the selected models may be biased because the ensemble mean of the selected models may overall overestimate or underestimate the TC activity compared to the whole CMIP6 dataset. For example, Lockwood et al. (2022) found that the climate models selected by Gori et al. (2022) to study the rain-surge joint hazard caused by US landfalling TCs overall project higher global temperature increase so it may overestimate TC activity. Thus, it is important to investigate which basic large-scale environmental parameters control modeled TC activity and develop a method for selecting a group of climate models based on their projection of these parameters to cover the range of TC activity change before performing climate downscaling. In this section, we aim to develop a statistical model that can help us predict the degree of changes in TC activities based on simple climate parameters.

PDI is developed by Emanuel (2005) and is used to represent TC activities and hazards (Emanuel 2005). PDI is first developed to represent TC wind hazard (Emanuel 2005), and it is also found to be a good indicator for TC rainfall hazard (Xi et al. 2023). PDI is the summation of the cube of storm intensity for each time step of all storms over a year in the basin, so it is influenced by both the simulated frequency and intensity of TCs. Inspired by the findings in Section 4, we use the low level (850 hPa) air temperature, high level (averaged between 300hPa and 500hPa) relative humidity, low level (850 hPa) vorticity and deep level (200 hPa – 850 hPa) wind shear (averaged during the TC season over the Atlantic basin) as predictors to the accumulated annual PDI in the Atlantic basin. We use these parameters because they are directly provided by CMIP6 climate models so that no additional calculations are needed, which would be required for Vp and SD, and these parameters cover both the dynamic and thermodynamic features of the climate condition. We aim to train a statistical surrogate model that links these parameters to the PepC downscaled TC yearly PDI. The reasons we train the statistical model based on PepC simulation results rather than historical observations are two-fold. First, as we aim to estimate the accumulated annual PDI based on the basin-wide averaged environmental field, we will only have less than 50 data points for historical observation, which is too few to train a neural-network model. PepC simulation outputs includes 10 Monte Carlo members of TCs downscaled from nine climate models since 1979 to 2100, the large dataset supports the training of a neural network model. Second, the purpose of developing the surrogate model is to help pre-select climate models before using PepC to downscale TC activities, so it is consistent to train the surrogate model based on PepC simulations. Researchers using other synthetic storm models to study TC climatology may consider training a similar model based on the chosen synthetic storm model.

While the complex relationship between TC activity and the basic environmental parameters cannot be captured by a linear model (not shown), we found that a shallow fully connected neural net is sufficient to predict annual PDI (results from test sets are shown in Figure 13a). The neural net has only one hidden layer and all nodes are connected with the output layer. The model is trained based on the 8-year moving average environmental parameters and PDI. The average window is selected to achieve good performance of the model in terms of distinguishing the degree of TC activity changes projected by different climate models while still including enough of the testing and validation data for model evaluation. The trained surrogate model is then fed with the 36-year averaged environmental parameters in historical (1979-2014) and future (2065-2100) climates simulated by each climate model. We show that the proposed statistical model can reproduce the wide range of projected change of TC activities shown in PepC simulations (Figure 13b). It may not exhibit good skill in distinguishing climate models that project relatively moderate change in storm activities, but it is skillful for finding the climate models that can project drastic or low changes in TC activity (CESM2, MPI, CANESM). The proposed statistical model thus can aid future research in TC downscaling by selecting the climate models that represent different degrees of TC climatology changes. The reason that the selected parameters can be used to approximately project the basin-wide TC activity is that the air temperature and relative humidity have strong influence on Vp and SD, which dominate the change of TC intensity and frequency (Section 4), while the wind shear and low-level vorticity have profound influences on the uncertainties across different climate models (Section 4).

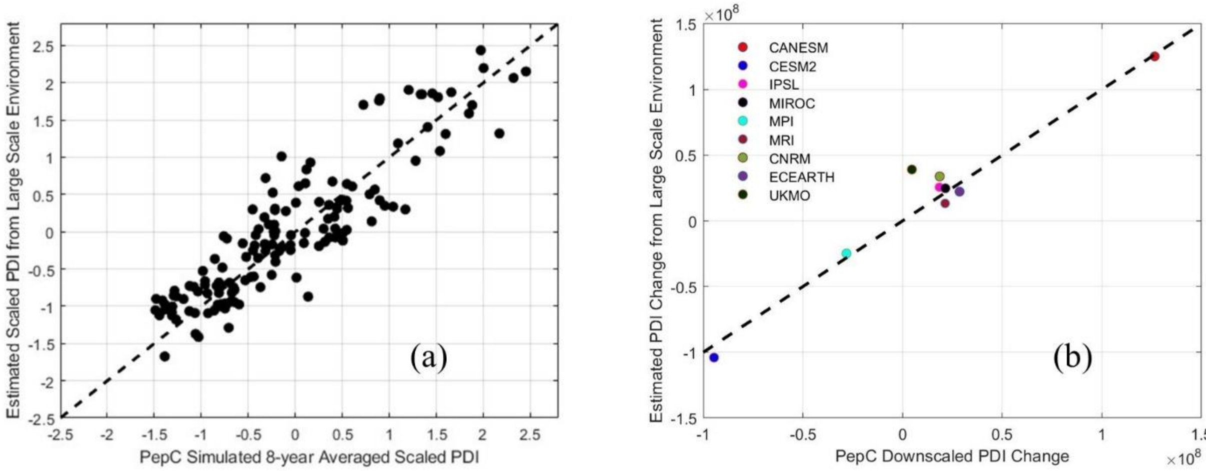

Figure 13. Approximate projection of basin-wide TC activity using the proposed simple statistical tool. (a) Estimated yearly (8-year moving averaged) PDI from the neural net compared with PepC downscaled PDI. The control simulation and SSP5 8.5 simulation from the nine climate models are used. Among all the available data, 75% of the data are chosen to train the model while the remaining 25% of the data are used as test set. Only the test set is plotted and the $R^2 = 0.68$. (b) Comparison between neural net estimated PDI change from 1979-2014 to 2065-2100 with PepC downscaled PDI change.

6. Discussions and Conclusions

In this study, we downscaled nine CMIP6 climate models using PepC to project TC activity change in the North Atlantic basin. We found that on average, TC frequency will decrease in the North Atlantic basin, consistent with most of previous research (Vecchi and Soden, 2007, Knutson et al., 2010, Villarini et al., 2011, Murakami et al. 2012) but differ from the statistical-dynamic downscaling of Emanuel (2021) and high-resolution climate simulation by Jing et al. (2021). We use saturation deficit as the humidity parameter for TC genesis prediction, and the results are consistent with the projection using saturation deficit in Lee et al. (2020). We found that TC intensity will increase in the future, consistent with most of previous studies (Emanuel 2005, 2013, 2021, Knutson and Tuleya, 2004, Murakami et al., 2012, Jing et al. 2021). Previous studies have also shown that the TC activity has been shifting poleward (Kossin et al. 2014) and will be shifting poleward in the future (Murakami et al. 2015), which is supported by the results of this study.

An important perspective that this study provides in addition to the projection of North Atlantic TC climatology is the understanding of why different climate models project different changes in TC activity. Using a synthetic TC model, we find the climate models have larger discrepancies/uncertainties in the projected changes in dynamic factors for TC activity, such as VO850 and Shear, than the projected changes in thermodynamic factors, such as Vp, SD and RH. In particular, this study emphasizes that the large spread in the projected Shear trend across models is the leading factor causing uncertainties in statistical climate projection of future TC activity. The uncertainties in the projection of Shear have been reported in previous studies and shown that they may be related to the uncertainties in TC activity projections (Camargo and Wing 2016, Murakami et al. 2017). This study, employing more climate models, further emphasizes the importance of understanding the uncertainties in the projection of wind shear for more reliably projecting future TC activity. The wide range of different projections of shear change may be related to the different projections of future meridional and zonal gradient of temperature in the climate models, which can be induced by the different parameterization of the surface physics, cloud feedback, and ice physics.

In the future, PepC will be coupled with more climate models under different scenarios (besides SSP5 8.5 used in this study) to project TC activity change. To better cover the range of climate projections, as a first attempt, we developed a statistical model that relates the large-scale environment (averaged air temperature, relative humidity, vorticity and wind shear) to TC activity (PDI). The developed statistical model can be used as a surrogate for screening climate models before calculating more complex parameters such as Vp and SD for downscaling simulations. It should be noted that the statistical surrogate model is built with TCs simulated by PepC, so it may not be suitable for other downscaling models. However, the ideas and methods can be easily transplanted to projections based on other downscaling models.

Acknowledgement:

The research is supported by the U.S. National Science Foundation (1652448 and 2103754 as part of the Megalopolitan Coastal Transformation Hub).

Data Availability Statement:

The CMIP6 simulation outputs can be found online in https/esgf-node.llnl.gov/projects/cmip6/. The downscale simulation results from PepC can be access online (link provided after acceptance)

Reference:

1. Balaguru, K., Chang, C.C., Leung, L., Foltz, G., Hagos, S., Wehner, M., Kossin, J., Ting, M. and Xu, W., 2023. A global increase in nearshore tropical cyclone intensification.

2. Bhatia, K., Vecchi, G., Murakami, H., Underwood, S. and Kossin, J., 2018. Projected response of tropical cyclone intensity and intensification in a global climate model. *Journal of Climate*, *31*(20), pp.8281-8303.

3. Camargo, S. J., & Wing, A. A. (2016). Tropical cyclones in climate models. *Wiley Interdisciplinary Reviews: Climate Change*, *7*(2), 211-237.

4. Chand, S.S., Walsh, K.J., Camargo, S.J., Kossin, J.P., Tory, K.J., Wehner, M.F., Chan, J.C., Klotzbach, P.J., Dowdy, A.J., Bell, S.S. and Ramsay, H.A., 2022. Declining tropical cyclone frequency under global warming. *Nature Climate Change*, 12(7), pp.655-661.

5. Emanuel, K. (2005). Increasing destructiveness of tropical cyclones over the past 30 years. *Nature*, *436*(7051), 686-688.

6. Emanuel, K., Ravela, S., Vivant, E. and Risi, C., 2006. A statistical deterministic approach to hurricane risk assessment. *Bulletin of the American Meteorological Society*, *87*(3), pp.299-314.

7. Emanuel, K. A. (2013). Downscaling CMIP5 climate models shows increased tropical cyclone activity over the 21st century. *Proceedings of the National Academy of Sciences*, *110*(30), 12219-12224.

8. Emanuel, K. (2021). Response of global tropical cyclone activity to increasing CO 2: Results from downscaling CMIP6 models. *Journal of Climate*, *34*(1), 57-70.

9. Flato, G., Marotzke, J., Abiodun, B., Braconnot, P., Chou, S. C., Collins, W., ... & Rummukainen, M. (2014). Evaluation of climate models. In *Climate change 2013: the physical science basis. Contribution of Working Group I to the Fifth Assessment Report of the Intergovernmental Panel on Climate Change* (pp. 741-866). Cambridge University Press.

10. Gori, A., Lin, N., Xi, D., & Emanuel, K. (2022). Tropical cyclone climatology change greatly exacerbates US extreme rainfall–surge hazard. *Nature Climate Change*, *12*(2), 171-178.

11. Hausfather, Z. and Peters, G.P., 2020. Emissions–the 'business as usual'story is misleading.

12. Jing, R., & Lin, N. (2019). Tropical cyclone intensity evolution modeled as a dependent hidden Markov process. *Journal of Climate*, *32*(22), 7837-7855.

13. Jing, R., & Lin, N. (2020). An environment-dependent probabilistic tropical cyclone model. *Journal of Advances in Modeling Earth Systems*, *12*(3), e2019MS001975.

14. Jing, R., Lin, N., Emanuel, K., Vecchi, G., & Knutson, T. R. (2021). A comparison of tropical cyclone projections in a high-resolution global climate model and from downscaling by statistical and statistical-deterministic methods. *Journal of Climate*, *34*(23), 9349-9364.

15. Karmalkar, A. V., Bradley, R. S., & Diaz, H. F. (2011). Climate change in Central America and Mexico: regional climate model validation and climate change projections. *Climate dynamics*, *37*, 605-629.

16. Knutson, T. R., McBride, J. L., Chan, J., Emanuel, K., Holland, G., Landsea, C., ... & Sugi, M. (2010). Tropical cyclones and climate change. *Nature geoscience*, *3*(3), 157-163.

17. Knutson, Thomas, et al. "Tropical cyclones and climate change assessment: Part II: Projected response to anthropogenic warming." *Bulletin of the American Meteorological Society* 101.3 (2020): E303-E322.

18. Knutson, T. R., & Tuleya, R. E. (2004). Impact of CO 2-induced warming on simulated hurricane intensity and precipitation: Sensitivity to the choice of climate model and convective parameterization. *Journal of climate*, *17*(18), 3477-3495.

19. Kossin, J. P., Emanuel, K. A., & Vecchi, G. A. (2014). The poleward migration of the location of tropical cyclone maximum intensity. *Nature*, *509*(7500), 349-352.

20. Lee, C. Y., Camargo, S. J., Sobel, A. H., & Tippett, M. K. (2020). Statistical–dynamical downscaling projections of tropical cyclone activity in a warming climate: Two diverging genesis scenarios. *Journal of Climate*, *33*(11), 4815-4834.

21. Lockwood, J. W., Oppenheimer, M., Lin, N., Kopp, R. E., Vecchi, G. A., & Gori, A. (2022). Correlation Between Sea-Level Rise and Aspects of Future Tropical Cyclone Activity in CMIP6 Models. *Earth's Future*, *10*(4), e2021EF002462.

22. Murakami, H., Vecchi, G. A., Villarini, G., Delworth, T. L., Gudgel, R., Underwood, S., ... & Lin, S. J. (2014). Seasonal Forecasts of Category 4 and 5 Hurricanes and Landfalling Tropical Cyclones using a High-Resolution GFDL Coupled Climate Model.

23. Murakami, H., Vecchi, G. A., Delworth, T. L., Wittenberg, A. T., Underwood, S., Gudgel, R., ... & Zhang, W. (2017). Dominant role of subtropical Pacific warming in extreme eastern Pacific hurricane seasons: 2015 and the future. *Journal of Climate*, *30*(1), 243-264.

24. Murakami, H., Vecchi, G.A., Underwood, S., Delworth, T.L., Wittenberg, A.T., Anderson, W.G., Chen, J.H., Gudgel, R.G., Harris, L.M., Lin, S.J. and Zeng, F., 2015. Simulation and prediction of category 4 and 5 hurricanes in the high-resolution GFDL HiFLOR coupled climate model. *Journal of Climate*, *28*(23), pp.9058-9079.

25. Murakami, H., Wang, Y., Yoshimura, H., Mizuta, R., Sugi, M., Shindo, E., ... & Kitoh, A. (2012). Future changes in tropical cyclone activity projected by the new high-resolution MRI-AGCM. *Journal of Climate*, *25*(9), 3237-3260.

26. Pithan, F., & Mauritsen, T. (2014). Arctic amplification dominated by temperature feedbacks in contemporary climate models. *Nature geoscience*, *7*(3), 181-184.

27. Sobel, A. H., Camargo, S. J., Hall, T. M., Lee, C. Y., Tippett, M. K., & Wing, A. A. (2016). Human influence on tropical cyclone intensity. *Science*, *353*(6296), 242-246.

28. Sobel, A. H., Wing, A. A., Camargo, S. J., Patricola, C. M., Vecchi, G. A., Lee, C. Y., & Tippett, M. K. (2021). Tropical cyclone frequency. *Earth's Future*, *9*(12), e2021EF002275.

29. Sugi, M., Murakami, H. and Yoshimura, J., 2009. A reduction in global tropical cyclone frequency due to global warming. *Sola*, 5, pp.164-167.

30. Ting, M., Kossin, J.P., Camargo, S.J. and Li, C., 2019. Past and future hurricane intensity change along the US East Coast. *Scientific reports*, *9*(1), p.7795.

31. Vecchi, G. A., & Soden, B. J. (2007). Global warming and the weakening of the tropical circulation. *Journal of Climate*, *20*(17), 4316-4340.

32. Villarini, G., Vecchi, G. A., Knutson, T. R., Zhao, M., & Smith, J. A. (2011). North Atlantic tropical storm frequency response to anthropogenic forcing: Projections and sources of uncertainty. *Journal of climate*, *24*(13), 3224-3238.

33. Woodruff, J. D., Irish, J. L., & Camargo, S. J. (2013). Coastal flooding by tropical cyclones and sea-level rise. *Nature*, *504*(7478), 44-52.

34. Xi, D., & Lin, N. (2022). Understanding uncertainties in tropical cyclone rainfall hazard modeling using synthetic storms. *Journal of Hydrometeorology*, *23*(6), 925-946.

35. Xi, D., Wang, S., & Lin, N. (2023). Analyzing relationships between tropical cyclone intensity and rain rate over the ocean using numerical simulations. *Journal of Climate*, *36*(1), 81-91.